Detailed Analysis of a Coaxial Stirling Pulse Tube Cryocooler with an Active Displacer

M. A. Abolghasemi[1], H. Rana[1], R. Stone[1], M. Dadd[1], P. Bailey[1], K. Liang[2]

[1]Department of Engineering Science, University of Oxford
Oxford OX1 3PJ, UK
[2]Department of Engineering and Design, University of Sussex
Brighton BN1 9RH, UK

ABSTRACT

Coaxial pulse tube cryocoolers are the configuration of choice as they allow better access to the cold head. Hence, a previously built and tested in-line pulse tube cryocooler which uses an active displacer for phase control has been modified into a coaxial configuration. The active displacer allows the mass flow and the pressure pulse at the cold end of the pulse tube to be easily adjusted for optimum performance. The displacer also allows the expansion power at the warm end of the pulse tube to be recovered in order to operate more efficiently. A numerical Sage model is used to examine the workflows throughout the cryocooler and it is shown that more than 6% of the power required to drive the cryocooler comes from the warm end of the pulse tube via the displacer. When using an inertance tube or orifice, this expansion power is dissipated as heat which is why using a displacer can lead to a more efficient cryocooler. Moreover, the recovered PV work via the displacer is measured and recorded experimentally.

INTRODUCTION

The operation of a Stirling Pulse Tube Cryocooler (SPTC) is governed by thermodynamic cycles using a working fluid, usually helium, that results in an intricate interplay between the pressure pulse and mass flow at the cold end to achieve cooling [1]. This is usually achieved via the use of an orifice or an inertance tube. However, Shi et al. [2] highlight that the phase angle between pressure and mass flow is difficult to freely adjust using orifices and inertance tubes. Alternatively, expanders (also known as phase shifters) and displacers can be used to ensure the correct relationship between mass flow and pressure. These allow for the phase to be adjusted more easily and allow for a wider range of phase angles to be investigated. The added benefit of a displacer (relative to an expander) is that it permits expansion power (PV power) to be recovered from the warm end of the pulse tube leading to a more efficient SPTC. SPTCs with displacers continue to be of interest as developers aim to increase the efficiency of their cryocoolers [3-4]. It is worth noting that although Stirling cryocoolers offer higher efficiencies in comparison to SPTCs, an SPTC with an ambient displacer is significantly less complicated to design and manufacture.

Displacers can be driven (i.e. active) or free moving (i.e. passive). SPTCs with active displacers present the further benefit of allowing for effortless fine-tuning of phase during operation for a more efficient cryocooler performance [5]. An active displacer is used in this study as it allows the optimum displacer phase and stroke values to be easily found while the SPTC is operating. This allows for a thorough experimental investigation of how the displacer dynamics affect the SPTC performance – especially the

Cryocoolers 21, edited by R.G. Ross, Jr., J.R. Raab and S.D. Miller

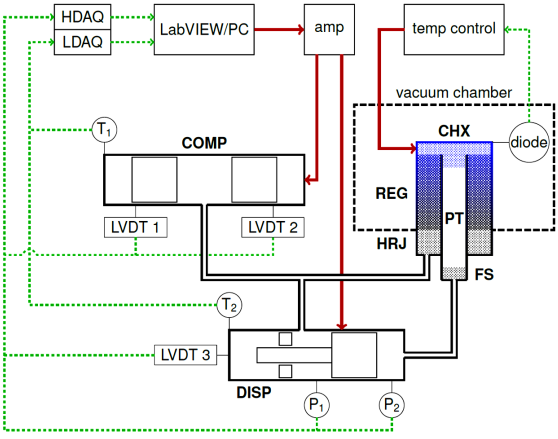

Figure 1. Coaxial SPTC experimental layout and instrumentation with abbreviations **COMP** for linear compressor, **DISP** for active displacer, **HRJ** for heat rejector, **REG** for regenerator, **CHX** for cold end heat exchanger, **FS** for flow straightener, **PT** for pulse tube, **HDAQ** for high speed data acquisition, **LDAQ** for low speed data acquisition, amp for amplifier, **T** for thermocouple and **P** for pressure transducer.

mass flow and pressure. This insight is extremely helpful when validating numerical models. Furthermore, once the optimum displacer dynamics are found, the spring stiffness and moving mass can be adjusted and the drive motor can be replaced with a suitable damper so that the active displacer is replaced by a passive one which operates at the optimum phase and stroke [6]. In other words, the active displacer paves the way to an efficient passive displacer design. In comparison, designing a passive displacer from scratch with no starting point would require far more design and testing iterations.

EXPERIMENTAL LAYOUT AND INSTRUMENTATION

Figure1 shows a schematic of the coaxial SPTC along with the instrumentation used. The cryocooler consists of:

- A dual piston oil-free linear compressor which acts as a pressure wave generator with a typical operating frequency of 60 Hz (COMP in Fig.1).
- An oil free single piston active displacer (DISP) operating at the same frequency as the linear compressor. The active displacer is a moving coil loudspeaker motor design where clearance seals around the displacer piston and shaft are maintained using flexure bearings. In this paper the expansion space to the right of the displacer piston is referred to as the displacer front volume and the space to the left of the displacer piston is referred to as the displacer back volume.
- An annular heat rejector at ambient temperature filled with copper mesh (HRJ).
- An annular regenerator filled with stainless steel mesh (REG).
- A cold end heat exchanger (CHX) designed to also act as a flow straightener. The cold end temperature was recorded using a silicon diode cryogenic temperature sensor; a small heater and a PID temperature controller were used to maintain a user-defined cold end temperature.
- A pulse tube (PT).
- A flow straightener at the warm end of the pulse tube filled with copper mesh (FS).

The compressor and displacer motion were controlled via user defined sinusoidal waveforms using LabVIEW. These were amplified and then delivered to the components. The displacements were monitored using linear variable differential transformer (LVDT) displacement transducers. Pressure transducers were also used to monitor the pressure either side of the active displacer. These data were recorded via a high speed data acquisition (HDAQ) card at a sampling rate of 5 kHz. Moreover, thermocouples were used to record component temperatures at a sampling rate of 10 Hz via a low speed data acquisition (LDAQ) card. Figure 2 shows a photo of the test setup.

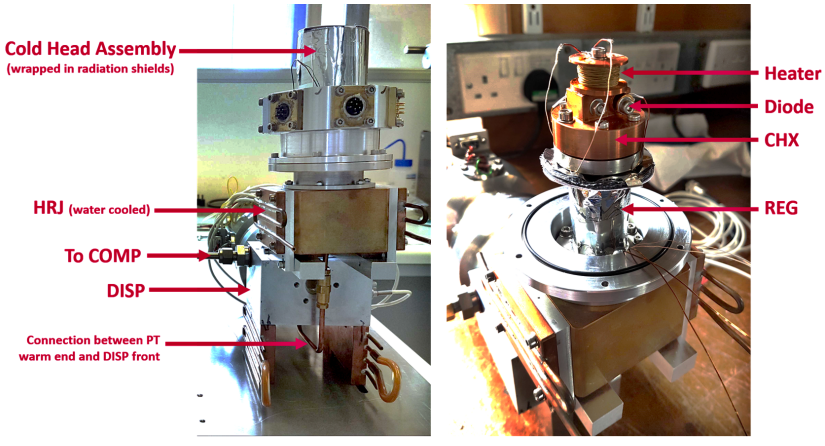

Figure 2. Photos of the coaxial SPTC showing (left) the lower half of the vacuum tank in place with radiation shields around the cold head and (right) radiation shields around the regenerator, with the cold head exposed. Abbreviations are the same as those described in Fig. 1.

SENSITIVITY TO DISPLACER PHASE AND STROKE

Optimum Values

By varying the active displacer motion relative to the linear compressor, the behaviour of the mass flow at the cold end can be altered. In order to assess the coaxial SPTC performance sensitivity to the displacer motion, several tests were carried out. These tests were carried out at a fill pressure of 28 bar and with an operating frequency of 60 Hz. During these tests, the cold end was maintained at 80 K and the cooling power was recorded. Initially, a constant displacer stroke of 4 mm was used and the displacer phase (relative to compressor motion) was increased from 30 ° to 60 °. Subsequently, a constant displacer phase of 45 ° was used and the displacer stroke was changed from 3.2 mm to 5.2 mm. A constant compressor stroke was used throughout. The results are shown in Fig. 3. Both cooling power and relative

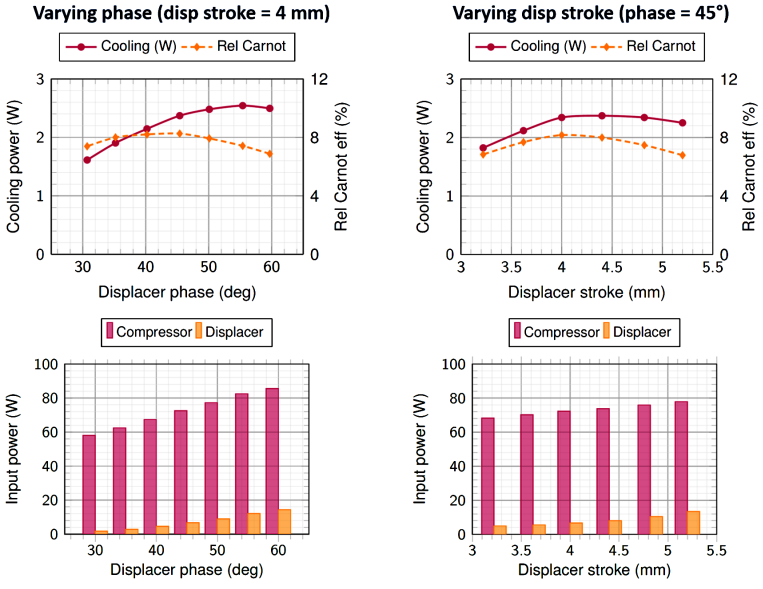

Figure 3. Coaxial SPTC performance sensitivity to active displacer phase and stroke with a fill pressure of 28 bar and an operating frequency of 60 Hz. A constant compressor stroke was used.

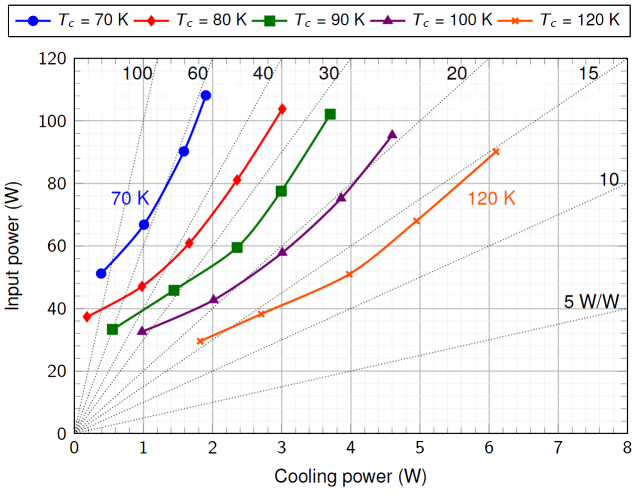

Figure 4. Coaxial SPTC performance at optimum displacer phase and stroke with a fill pressure of 28 bar and an operating frequency of 60 Hz. Lines of constant specific power (in W/W) are shown.

Carnot efficiency are shown. Compressor and displacer contributions to total input power during the displacer phase and stroke sensitivity experiments are also shown.

The results reveal optimum values for both displacer phase and stroke. The phase sensitivity plot suggests an optimum phase value of around 55 º for maximum cooling power. Optimum efficiency occurs at a lower value of 45 º. In terms of displacer stroke, maximum cooling power occurs at around 4.4 mm with maximum efficiency at around 4 mm. Noticeably, the peaks in both plots are broad and this suggests that a small deviation away from the optimum phase and stroke values will not have a significant effect on the SPTC performance.

Performance at Optimum

Having discovered the optimum displacer stroke and phase values, further tests were carried out to map the SPTC performance at different cold end temperatures ranging from 70 K to 120 K. For these tests a constant displacer phase values of 45 º and a constant displacer stroke value of 4 mm was used. These were the optimum values in terms of highest efficiency at 80 K (see Fig. 3). The fill pressure was 28 bar and the operating frequency was 60 Hz. The results are shown in Fig. 4.

WORKFLOWS

In order to better understand the operation of the SPTC performance a numerical Sage model [7] of the coaxial SPTC was created. The values for the reference temperatures in the Sage model were set to the values recorded via thermocouples in the experiments. The Sage model allows for an in depth look into the workflows within the SPTC. The cyclic average enthalpy flows along with the heat transfers into or out of each component are shown in Fig. 5. The PV powers into or out of the compression space, the displacer front and back spaces are also shown. The values shown are for the optimum operating conditions with displacer phase of 45° and stroke of 4 mm. This workflow demonstrates the ability of the displacer to recycle the expansion work from the warm end of the pulse tube. According to Sage, out of the 69 W of enthalpy flowing into the heat rejector (which is essentially driving the cryocooler), 4.5 W is coming from the displacer.

Note that according to Fig. 5 the regenerator transfers 3.5 W of enthalpy from its warm end to the cold head whereas in the ideal case there would be no enthalpy flow down the regenerator. Furthermore, less than 80% of the 7 W of enthalpy from the cold head is delivered to the displacer. This suggests that the flow straightener is acting as a heat exchanger. Ideally one would not want any of the expansion power to be rejected as heat, but it is difficult to isolate the flow straightener given its proximity to the heat rejector.

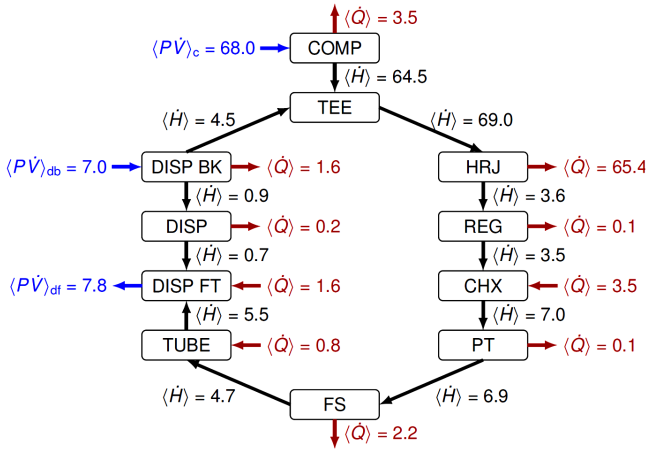

Figure 5. Cyclic averaged enthalpy flows (black), PV powers (blue) and heat flows (red) according to Sage in units of W. Abbreviations are the same as those described in Fig. 1 plus **DISP FT** and **DISP BK** for displacer front and back volumes, respectively. Also, **TEE** is the T junction where the output from the displacer is connected back into the cycle. Results shown are for the optimum operating conditions with displacer phase of 45° and stroke of 4 mm.

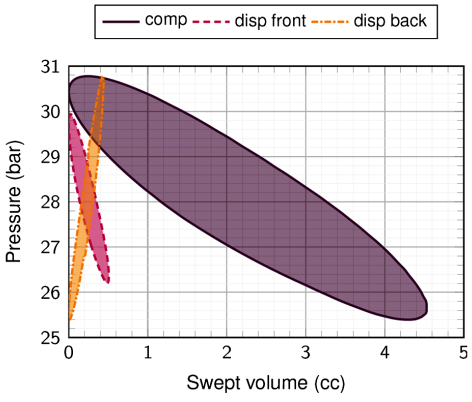

Figure 6. Experimental PV plots using pressure measurements and LVDT data at optimum operating conditions with displacer phase of 45° and stroke of 4 mm.

PV POWERS

The PV powers are also of interest because although the enthalpy flows of the real system are not available, PV powers can be computed using the experimental pressure measurements and the LVDT displacement data. Figure 6 shows the experimental PV plots for the compression space and the displacer front and back spaces. The plot shown corresponds to the optimum operating conditions with displacer phase of 45° and stroke of 4 mm. According to the experimental data, the PV powers are 52 W in the compression space and 3.7 W in both the displacer front and back spaces. These values are smaller than those predicted by Sage (see Fig. 5), but the proportions of recycled expansion PV power ($<P\dot{V}>_{db}$) to compressor input PV power ($<P\dot{V}>_{c}$) are in broad agreement with the Sage model predicting 10% and the experimental data indicating 7%.

In the future, the active displacer will be replaced by a passive one. For the displacer to operate passively, the extracted PV power from the front space must match the PV power going into the back space. In reality the extracted PV power must be slightly larger in order to overcome friction, but since there is a clearance between the displacer piston and the surrounding cylinder, the frictional losses will be relatively small.

CONCLUSIONS

This study focused on the performance optimisation and detailed analysis of a coaxial SPTC with an active displacer. The key findings are:

1. The active displacer allows the performance of the SPTC to be easily optimised during operation by varying the displacer motion relative to the compressor.
2. The displacer can recycle some of the expansion power from the warm end of the pulse tube back into the cycle and it is shown that 6% of the power required to drive the cryocooler comes from the displacer. This can help produce a more efficient SPTC compared to the commonly used inertance tube SPTC.
3. The flow straightener is acting as a heat exchanger and if this is resolved more work can be recovered.
4. With the optimal phase and stroke now known, the active displacer can be replaced with a passive one leading to higher efficiencies and a more compact design.

ACKNOWLEDGMENT

The authors acknowledge the support of Honeywell Hymatic during the design and manufacture of the SPTC. The authors further acknowledge support from the EPSRC under research project EP/N017013/1.

REFERENCES

1. Radebaugh, R., "Development of the Pulse Tube Refrigerator as an Efficient and Reliable Cryocooler," *Proceedings of Institute of Refrigeration,* vol 96 (2000), pp. 11-29.
2. Shi, Y., Zhu, S., "Experimental investigation of pulse tube refrigerator with displacer," *International Journal of Refrigeration*, vol. 76 (2017), pp. 1-6.
3. M. Wang, H. Xu, Y. Lin, Z. Zhang, S. Zhu, "Experimental investigation of pulse tube refrigerator with rod type displacer as phase shifter," *International Journal of Refrigeration*, vol. 93, no. 47 (2018), pp. 47-51.
4. A. de Waele, "Pulse-tube refrigerator with a warm displacer: Theoretical treatment in the harmonic approximation," *Cryogenics*, vol. 100 (2019), pp. 53-61.
5. M. A. Abolghasemi, H. Rana, R. Stone, M. Dadd, P. Bailey, K. Liang, "Coaxial Stirling pulse tube cryocooler with active displacer," *Cryogenics*, vol. 111 (2020).
6. H. Rana, M. A. Abolghasemi, R. Stone, M. Dadd, P. Bailey, "Numerical modelling of a coaxial Stirling pulse tube cryocooler with an active displacer for space applications," *Cryogenics*, vol. 106 (2020).
7. Gedeon, D., "Sage: Object-Oriented Software for Cryocooler Design," *Cryocoolers 8,* Plenum Press, New York (1995), pp. 281-292.